Reproductive Sciences (2022) 29:1471–1485
https://doi.org/10.1007/s43032-022-00844-y

MALE REPRODUCTION: ORIGINAL ARTICLE

Acute and Chronic Exposure to 900 MHz Radio Frequency Radiation Activates p38/JNK-mediated MAPK Pathway in Rat Testis

Hakan Er[1,2] · Gizem Gamze Tas[3] · Bikem Soygur[3,4] · Sukru Ozen[5] · Leyla Sati[3]

Received: 28 September 2021 / Accepted: 1 January 2022 / Published online: 11 January 2022
© Society for Reproductive Investigation 2022

Abstract

The use of electronic devices such as mobile phones has had a long stretch of rapid growth all over the world. Therefore, exposure to radio frequency radiation (RFR) has increased enormously. Here, we aimed to assess the balance between cell death and proliferation and also investigate the involvement of the JNK/p38 MAPK signaling pathway in the testis of rats exposed to 900 MHz RFR in acute and chronic periods (2 h/day, 5 days/week) for 1 or 10 weeks, respectively. The expression of proliferating cell nuclear antigen (PCNA), Bcl-xL, cleaved caspase-3, phosphorylated-JNK (p-JNK), and phosphorylated-p38 (p-p38) was analyzed in line with histopathology and TUNEL analysis in rat testis. There were no histopathological differences between sham and RFR groups in the acute and chronic groups. PCNA expression was not altered between groups in both periods. However, alterations for cleaved caspase-3 and Bcl-xL were observed depending on the exposure period. TUNEL analysis showed a significant increase in the RFR group in the acute period, whereas no difference in the chronic groups for the apoptotic index was reported. In addition, both p-p38 and p-JNK protein expressions increased significantly in RFR groups in both periods. Our study indicated that 900 MHz RFR might result in alterations during acute period exposure for several parameters, but this can be ameliorated in the chronic period in rat testis. Here, we also report the involvement of the p38/JNK-mediated MAPK pathway after exposure to 900 MHz RFR. Hence, this information might shed light in future studies toward detailed molecular mechanisms in male reproduction and infertility.

Keywords Radio frequency radiation · Rat · Testis · p38 · JNK

Introduction

In recent years, human exposure to RFR has increased dramatically due to the widespread use of electronic devices, particularly mobile phones [1]. In fact, the current smartphones are not only for talking to each other, but they also offer some of the similar features that a personal computer or a TV would, resulting in increased digital screen time for individuals. To perform these operations, they must be constantly connected to the base stations. However, they receive and emit RFR while they are working. An important consideration in this context is the possible effects of these devices on human health [2, 3]. While the pathophysiological mechanisms underlying the potential health effects associated with RFR due to mobile phones or similar electronic devices are not well understood, the International Agency for Research on Cancer (IARC) has classified RFR as a possible carcinogen for humans [4–6]. In relation to the amount and duration of exposure to RFR, there are no definitive standards for the emergence of negative health effects on

✉ Leyla Sati
leylasati@yahoo.com

1 Department of Biophysics, Akdeniz University School of Medicine, Akdeniz University, Antalya, Turkey

2 Department of Medical Imaging Techniques, Vocational School of Health Services, Akdeniz University, Antalya, Turkey

3 Department of Histology and Embryology, Akdeniz University School of Medicine, Campus, 07070 Antalya, Turkey

4 Department of Obstetrics, Gynecology and Reproductive Sciences, Center for Reproductive Sciences, Eli and Edythe Broad Center of Regeneration Medicine and Stem Cell Research, University of California San Francisco, San Francisco, CA, USA

5 Department of Electrical and Electronics Engineering, Faculty of Engineering, Akdeniz University, Antalya, Turkey

the human body. Thereafter, investigations on the biological effects of RFR have increased dramatically in recent years, and many of the studies reported conflicting results. Some studies concluded that there were no adverse effects [7, 8]; however, some of the studies indicated effects such as testicular cell apoptosis [9], glioma formation [10], DNA damage in germ cells leading to low sperm count [11] and lower sperm quality [12].

One of the most important effects of RFR is that it causes oxidative stress by increasing the level of free radicals and their cleaning durations from the environment [13]. Thus, the rate of free radical formation in the organism and the rate of their removal from the intracellular and extracellular environment is kept in a critical balance for proper physiological functions [14, 15]. However, in cases where free radical production exceeds the capacity of the antioxidant defense system, this equilibrium is disrupted, and increased free radicals react with lipids, especially DNA, protein, and carbohydrates, causing damage to the structural and functional integrity of the cell [16].

Oxidative stress, together with increased reactive oxygen species (ROS), may cause stress-mediated damage to the cells, tissues, and organs [17–20]. ROS formation is essential for normal fertilization and plays an important role in many physiological processes in the male reproductive system including sperm capacitation and hyperactivation [21–23]. However, excessive ROS production can also cause sperm dysfunction through lipid peroxidation, loss of motility, and DNA damage leading to pathological consequences [22, 24, 25]. Previous studies reported that RFR can affect male fertility since it causes DNA damage, oxidative stress, and a significant decrease in testicular weight, seminiferous tubules, and sperm count [12, 26–28]. Affected parameters include sperm concentration, motility, morphology, viability, and sperm apoptosis [27, 29–31]. Therefore, it has been suggested that carrying mobile phones close to the testis can reduce sperm quality [32].

Oxidative stress is known to induce apoptosis in cells by affecting intracellular signaling pathways [33]. Activation of mitogen-activated protein kinases (MAPKs) is critical in the oxidative stress-mediated apoptosis-associated signaling pathway [34]. MAPKs are serine and threonine protein kinases that are translocated to the nucleus after activation by external stimuli such as hormones, growth factors, carcinogenic substances, osmotic stress, radiation, and inflammation [35, 36]. The MAPK pathway may involve different biological responses such as cell division, differentiation, migration, gene expression, and apoptosis [37–40]. MAPK family is divided into three main groups as p38 MAPK, extracellular signal-regulated kinase (ERK), and c-Jun NH2-terminal kinases (JNKs) [41, 42]. ROS-induced oxidative stress has been shown to activate MAPK members by phosphorylation [11, 43]. Studies have shown that ERK1 and ERK2 are activated by growth stimuli and promote cell growth, whereas JNK and p38 MAPKs are activated in response to various environmental stresses and inflammatory signals and promote apoptosis and growth inhibition [40, 44–49]. Therefore, both JNK and p38 MAPKs are considered to be stress-activated protein kinases (SAPK) [38, 39]. Many isoforms of ERK, JNK, and p38 MAPK are present in the mammalian testis and expressed by Sertoli and germ cells, playing crucial roles during spermatogenesis [50–55]. MAPK activity is also important for the mobilization of sperm during the epididymal transition and fertilization of oocytes [56]. Although it is still unclear how the JNK/p38 MAPK signaling pathway affects cellular survival or death, the current literature suggests that the JNK/p38 MAPK cascade may involve in cellular responses to ROS. Therefore, in the current study, we aimed to investigate the cell death and proliferation balance in rat testis due to 900 MHz RFR exposure in acute and chronic periods and also determine whether or not JNK/p38 MAPK signaling pathway is affected.

Materials and Methods

Experimental Groups

Three-month aged male albino Wistar rats, weighing between 250 and 300 g, were used in the experiment [57]. Twenty-four Wistar rats were randomly divided into 4 groups ($n = 6$/group); the sham group for 1 week (S1), the sham group for 10 weeks (S10), 900 MHz RFR group for 1 week (RFR1), and 900 MHz RFR group for 10 weeks (RFR10). Rats in the RFR1 group were kept in plexiglass tubes for 2 h/day for 1 week (5 days). Rats in the RFR10 group were kept in plexiglass tubes for 2 h/day and 5 days/week for 10 weeks. Acute and chronic sham group rats were kept in the same room, under the same conditions and equal time periods with RFR groups during the experiment. In the experiments, the RF stimulator was kept in the OFF mode for the sham groups and in the ON mode for the RFR groups. Various RFR exposure periods have been carried out on experimental animals in RF studies in the literature [9, 58, 59]. However, we studied 2 h/day and 5 days/week as RFR exposure period similar to the study published by Ammari M. et al. [60]. In our study, we have created 1 and 10 weeks of groups to determine the short and long-term effects of RFR. During the test periods, animals were kept in a 12 h light/dark cycle with 4 rats in each cage, and the animals were fed with commercial rat feed and tap water. Figure 1A shows the timeline of the experimental setup for sham and 900 MHz RFR groups in acute and chronic periods.

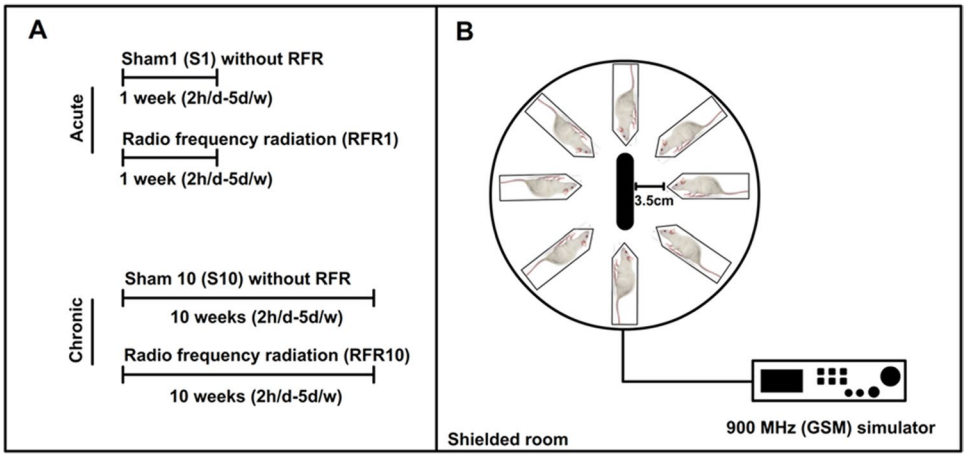


Fig. 1 Experimental timeline (**A**) and RFR exposure setup (**B**) are presented

Radio Frequency Radiation Application

The RF value used in this study is the frequency used in 900 MHz mobile phone communication. An RF generator (GSM Simulator 900 MHz; Everest Company, Adapazari, Turkey), which produces 900 MHz RF radiation, was used to represent the exposure of global systems for mobile communications (GSM). The carrier frequency was 900 MHz, the modulation frequency was 217 Hz, the pulse width was 0.577 ms, and the power range of the generator was 0–10 W.

The animals were placed in plexiglass tubes with holes where one single rat could fit, breathe comfortably, and not increase the body temperature (Fig. 1B). Rats in plexiglass tubes were placed radially at equal distances (rats' noses were at 3.5 cm distance from the antenna) around the antenna. The applied carousel setup procedure of the present study was in accordance with the setup procedure of the other studies in the literature [61–63]. The tubes restrained the movement of the rats to such an extent as to follow for well-defined exposure conditions yet without immobilizing them. RFR application was held in a shielded room in order to prevent the rats from the effects of other electrical sources. For the used frequency, the source output powers were selected by considering the power values emitted by the mobile phones (the output power adjusted to 5 W during the exposure). During the experiment in the "signal on" situation, the measured electric field strengths over the rats' heads positioned 3.5 cm away from the antenna were 35.5 V/m for 900 MHz. Besides, the RFR device was controlled every day during the experiments whether it was processing properly. Electric field strengths were measured by EMR300 (Narda, Germany) with a suitable probe in the experiment. The electric field background level was between 0.02 and 0.2 V/m in the shielded room. Also, the background magnetic field was measured between 0.01 and 0.03 μT by Hioki 3470 Magnetic Field HiTESTER (Hioki E. E. Corp., Japan) with an appropriate probe.

Dosimetry simulations were carried out using a finite integration technique (FIT) based commercial software, CST Microwave Studio (3DEXPERIENCE®, Dassault Systèmes, Hamburg). The FIT was introduced by Weiland [64]. Although the gridding can be applied as a finite difference time domain (FDTD) method, the FIT uses the integral form of Maxwell's equations [65]. In the present study, the rat model used in simulations has consisted of voxels with a resolution of $1.827 \times 1.827 \times 2.015$ mm^3. The interaction between the incident electromagnetic wave and the biological tissue are explained by electrical properties that can be obtained by the dielectric properties of the interested tissue [66, 67]. In this study, each tissue of the simulated rats has its electrical properties at the operating frequencies. The average whole-body SAR value at 900 MHz was 1.159 W/kg. The SAR value for the testes was on the average of 0.107 W/kg. Prior to and after all experimental sessions, the body temperatures of rats were monitored by rectal measurements. The RFR exposure did not lead to any rectal temperature raise.

Tissue Collection

At the end of the experiments, testis tissues were dissected from rats. A routine tissue follow-up protocol was applied in our laboratory by fixation in Bouin solution for 4 h at room temperature. Following washing in tap water, tissues were passed through increasing series of ethanol (70%, 80%, 90%, and 100%) for dehydration. Testis tissues were processed in 100% ethanol for 4 h. After the dehydration process, the tissue samples were made transparent with xylol application. Paraffinization was performed by keeping the tissues in three series of paraffin for 1 h each in a 60 °C drying oven and then embedded in paraffin wax for immunohistochemistry [68]. By using a rotary microtome (Leica RM2125 RTS), 5-μm-thick serial sections from the blocks were taken on positively charged

slides. One testis was used for histopathology and immunohistochemistry, whereas the other testis tissue was snap frozen in liquid nitrogen for Western blot analysis.

Testicular Histopathology

Possible effects of 900 MHz RFR exposure on testis in acute and chronic periods were evaluated histopathologically. In order to analyze the testicular structure better, periodic acid-Schiff (PAS) staining was performed on sections after deparaffinization. For PAS staining, 5-µm-thick sections taken from paraffin blocks were kept in an oven at 60 °C overnight and passed through the xylol and alcohol series. The slides were then passed through tap water, oxidized in 1% periodic acid (H5IO6) for 5 min, and then rinsed in 70% alcohol. They were treated in Shiff solution for 5–45 min and then washed under running water, then stained with Hemaloun for 30 s, and washed under running water. Finally, the slides were passed through alcohol series and xylol and closed with Entellan. Developmental stages of the seminiferous epithelium in cross sections of testis were identified according to the criteria previously described [69]. Considering this description of the cycle of the seminiferous epithelium may serve as the basis for histophysiological investigations of the rat testis. Periodic acid-Schiff stain is necessary to stain the glycoprotein component of the acrosome and allow accurate identification of all 14 stages of the seminiferous cycle [70]. However, the stages for the seminiferous tubules were pooled according to the classification used in previous toxicity studies and literature as stages I–V, stages VI–VIII, and stages IX–XIV. Since, with practice, recognition of stages is complicated in preparations counterstained with only hematoxylin as used in immunohistochemistry protocols [71].

Immunohistochemistry

Immunohistochemical staining of PCNA, Bcl-xL, cleaved caspase-3, p-JNK, and p-p38 proteins were performed in paraffin sections from testis samples. PCNA expression was used as a marker of cell proliferation since the cells remain a long time in the G1/S phase when proliferating. Bcl-xL is a member of anti-apoptotic BCL-2 family proteins. On the other hand, cleaved caspase-3 was studied as a marker of apoptosis. JNK and p38 MAPKs were also included as they were considered to be SAPKs. Serial sections at 5-µm thickness were collected on poly-L-lysine-coated slides (Sigma, St. Louis, MO), dewaxed, rehydrated, and placed in citrate buffer. To unmask antigens, an antigen-retrieval procedure was performed by treating the samples in a microwave oven at 750 W for 5 min twice. After cooling for 20 min at room temperature, the sections were washed in PBS and then kept in 3% H2O2 for 15 min to remove endogenous peroxidase activity, followed by three washes with PBS. After blocking with Ultra V blocking reagent (Lab Vision, Fremont, CA) for 10 min at room temperature to reduce non-specific binding, the primary antibodies were incubated overnight at +4 °C in a humidified chamber (Table 1). The sections were washed three times in PBS and incubated with related secondary antibodies for 45 min at room temperature (Table 1). After three times of washes with PBS, the antigen-antibody complexes were detected by using a streptavidin-peroxidase complex (TP-125-HL; Lab Vision, Fremont, CA, USA) for 15 min followed by three rinses in PBS. The resulting signal was developed with diaminobenzidine (DAB) tablets (D-4168; Sigma Aldrich, MO, USA), and the sections were counterstained with Mayer's hematoxylin (1.09249.1000; Merck, Darmstadt, Germany) and mounted on glass slides. For isotype controls, sections were treated with either appropriate mouse IgG2a or normal rabbit IgG, depending on the primary antibody used and diluted to the same protein concentration as the primary antibody. Photomicrographs were

Table 1 Primary and secondary antibody dilutions used for immunohistochemistry and Western blot methods

		Company/catalog no.	IHC Dilution	Western blot Dilution
Primary antibodies	PCNA	Cell Signaling #2586S	1:600	1:1000 (in TBS-T)
	Bcl-xl	Cell Signaling #2764S	1:300	1:1000 (in TBS-T)
	Cleaved caspase-3	Cell Signaling # 9661S	1:300	1:500 (in TBS-T)
	Phosphorylated-JNK (p-JNK)	Thermo Fisher Scientific #44682G	1:200	1:1000 (in 5% nonfat dry milk)
	Phosphorylated-p38 (p-p38)	Cell Signaling #4511S	1:100	1:500 (in 5% nonfat dry milk)
	Beta-actin	Santa Cruz Biotechnology Inc. #sc-47778		1:4000 (in 5% nonfat dry milk)
Secondary antibodies	Biotinylated anti-rabbit	Vector Laboratories #BA-1000	1:400	
	Biotinylated anti-mouse	Vector Laboratories #BA-2000	1:400	
	HRP-conjugated anti-rabbit	Vector Laboratories #PI-1000		1:2000 (in 5% nonfat dry milk)
	HRP-conjugated anti-mouse	Vector Laboratories #PI-2000		1:2000 (in 5% nonfat dry milk)

taken with an Axioplan microscope (Zeiss, Oberkochen, Germany) using Spot Imaging software version 4.6 (Diagnostic Instruments, Inc.). All samples for each individual antibody were exposed to the same protocol at the same time and were stained using the same incubation periods. In addition to the localization patterns, which have been compared to reported studies in the literature, the threshold analysis of the IHC images for each staining was also assessed by using ImageJ version 1.46 (NIH) particularly on stage matched seminiferous tubule sections and graphed for both sham and 900 MHz RFR groups in acute and chronic periods.

SDS-PAGE and Western Blotting

Total protein from rat testes was extracted with cell extraction buffer (Thermo Fisher Scientific BioSource International; Camarillo, CA) containing 3 mM phenylmethylsulfonyl fluoride (PMSF) and protease inhibitor cocktail (P8340; Sigma-Aldrich, MO, USA). The protein concentration was determined by a detergent compatible protein assay (Bicinchoninic Acid Kit for Protein Determination BCA1-1KT Sigma). Samples (50 µg) were loaded on 10% Tris–HCl gels, electrophoretically separated, and electroblotted onto PVDF membrane (Bio-Rad Laboratories, CA, USA). The membranes were blocked with 5% nonfat dry milk in TBS containing 0.1% Tween 20 (TBS-T) for 1 h to reduce nonspecific binding. The membranes were incubated overnight at +4°C with primary antibodies (Table 1). After primary antibody incubation, the membranes were washed in TBS-T for 1 h and incubated with horseradish peroxidase-conjugated secondary antibodies, listed in Table 1, for 1 h at room temperature. The protein was visualized by light emission on film (Amersham Biosciences; Buckinghamshire, England), and the signal was detected using SuperSignal Chemiluminescent kit (34080; Thermo Fisher Scientific, USA) and quantified. The rat testis extracts were prepared. As the internal control to confirm the equal loading of the samples, a β-actin antibody (Table 1) was used for 2 h at room temperature to probe each immunoblot simultaneous to the probe for antibody probes. The relative levels of proteins were quantified by optical density analysis using ImageJ version 1.46 (NIH). The optical density (OD) values of bands were normalized to the OD values of β-actin bands and then graphed.

Terminal Deoxynucleotidyl Transferase dUTP Nick End Labeling (TUNEL) Assay

Testicular cell apoptosis in the testis sections was detected by enzymatic labeling of DNA strand breaks using terminal deoxynucleotidyl transferase-mediated TUNEL. In situ nick end labeling of nuclear DNA fragmentation was performed in a humid chamber for 1 h in the dark at 37 °C with a commercially available TUNEL kit (In situ Cell Death Detection Kit, AP, Roche Diagnostics, 1684809; Mannheim, Germany), at a dilution of 1:2 in reaction buffer. Slides were fixed for 20 min in 4% paraformaldehyde at room temperature. Samples were washed in PBS and treated with permeabilization solution (0.1% Triton X-100 in 0.1% sodium citrate) for 5 min on ice. After washing with PBS, the labeling reaction was performed using 50 ml TUNEL reagent to each sample, except the negative control, in which reagent without enzyme was added and incubated for 1 h at 37 °C at dark. Following PBS washings, slides were incubated with converter reagent for 30 min at 37 °C, subsequently, color development for localization of cells containing labeled DNA strand breaks was performed by incubating the slides with Fast Red substrate solution for 5 min. Slides were mounted with a permanent mounting medium.

TUNEL staining method was used to determine apoptotic index in the testis sections of sham and 900 MHz RFR groups. Thus, TUNEL-positive and TUNEL-negative seminiferous tubules were defined in each group. Seminiferous tubules with apoptotic cell signals were identified as positive seminiferous tubules. The ratio of positive tubules to total tubules was multiplied by 100 and apoptotic index (%) of seminiferous tubules was calculated. Cell and seminiferous tubule stage-specific apoptotic effects of exposure to 900 MHz RFR were also evaluated in acute and chronic periods.

Statistical Analysis

The mean values, standard deviations, and median values for the experimental data were calculated using descriptive statistics. Results were expressed as the mean ± SEM. The quantitative data was submitted to normality tests by the Kolmogorov–Smirnov test. Data were compared using one-way ANOVA followed by Holm–Sidak post hoc test for the data passed the normality test, otherwise, the Kruskal–Wallis test was followed by Dunn's test (SigmaStat® 3.5 program, Jandel Corporation, San Rafael, CA). The results of acute and chronic periods were compared with the sham groups of the related week and determined whether there were any significant differences between the groups. p values < 0.05 among different groups were considered statistically significant.

Results

Testicular Histopathology After Exposure to 900 MHz RFR in Acute and Chronic Periods

Seminiferous tubules and interstitial cells were evaluated by PAS staining in testicular sections from sham and 900 MHz RFR groups in acute and chronic periods. Leydig cells,

tubule basement membranes, and acrosome structures were clearly analyzed in all groups by PAS staining. However, there were no significant differences attributable to exposure to 900 MHz RFR noted in histopathology and seminiferous tubule stages for acute and chronic periods (Fig. 2).

Testicular Cell Proliferation After Exposure to 900 MHz RFR in Acute and Chronic Periods

PCNA positive cells were observed extensively in spermatogonial cells and spermatocytes with a nuclear staining pattern in all tubule stages as expected (Fig. 3). No differences were observed between acute or chronic RFR groups with respect to their sham groups in terms of PCNA localization pattern (Fig. 3). In addition, there were no differences in PCNA staining intensity between sham and RFR groups in both acute and chronic periods according to the ImageJ threshold analysis.

Besides, Western blot analysis of PCNA (36 kDa) protein with testicular lysates showed statistically similar data that PCNA expression levels were not altered between sham and RFR groups in both acute and chronic periods (Fig. 7).

Apoptotic Cell Death in Testis Tissues After Exposure to 900 MHz RFR in Acute and Chronic Periods

Cleaved caspase-3 immunoreaction was detected in postmeiotic germ cells, especially round spermatids (Fig. 3). The staining pattern was particularly observed in the VI–VIII tubule stages. No differences were observed between sham and RFR groups in terms of cleaved caspase-3 immunolocalization pattern (Fig. 3). Furthermore, the ImageJ threshold analysis also revealed that there were no significant differences for cleaved caspase-3 stainings in RFR groups when compared to their sham groups in the acute and chronic periods.

Western blot analysis of cleaved caspase-3 (19 kDa) protein in testicular tissues revealed similar observations that cleaved caspase-3 protein expression level was not statistically different in the RFR group when compared to its sham group in the acute period (Fig. 7). However, a statistically significant decrease in cleaved caspase-3 expression was measured in the RFR group with respect to its sham group in the chronic period ($p < 0.027$) (Fig. 7).

On the other hand, Bcl-xL immunostaining, as a critical antiapoptotic protein, was widely expressed in the cytoplasmic areas of spermatocytes and round spermatids (Fig. 3). Its presence in elongated spermatids and mature spermatozoa released from Sertoli cells into the seminiferous tubule lumen have also been identified. This cellular staining pattern was observed similarly in all groups. However, there was a significant decrease ($p < 0.001$) in the RFR group for Bcl-xL staining in the acute period, whereas no difference in the chronic period with respect to its sham group according to ImageJ threshold analysis was detected.

In line with IHC, similar data were obtained with Western blot analysis that there was a statistically significant decrease in Bcl-xL (25 kDa) expression in the RFR group with respect to the sham group in the acute period ($p < 0.005$) in contrast to no statistically significant difference between groups in the chronic period (Fig. 7).

In addition to cleaved caspase-3 and Bcl-xL immunostainings, we also performed a TUNEL assay to detect apoptotic tubule index (%) after exposure to 900 MHz RFR

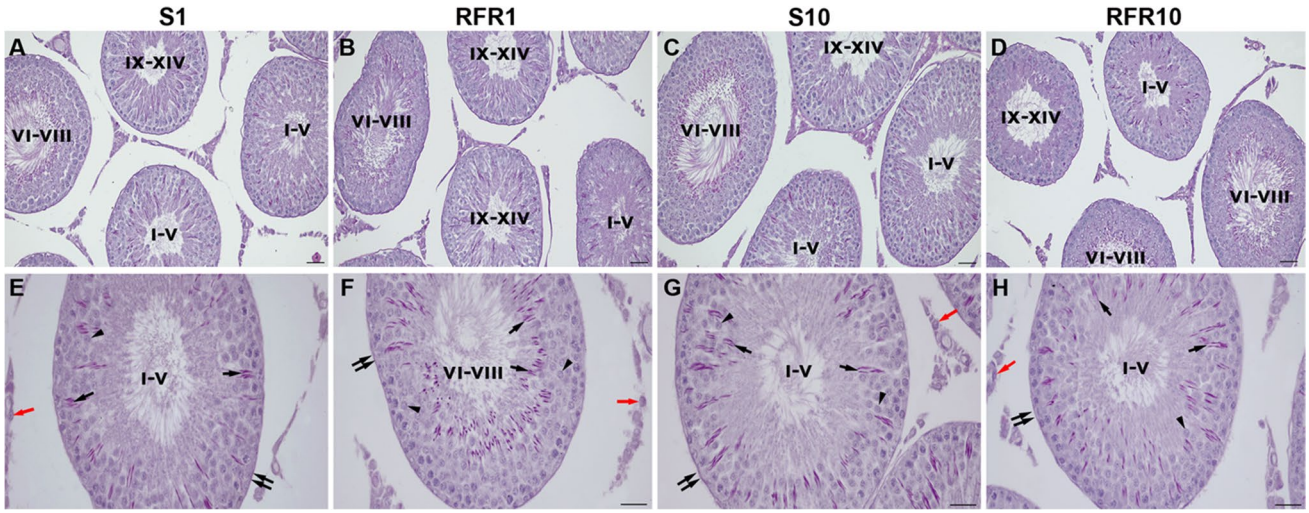


Fig. 2 PAS staining in testicular tissues from sham and 900 MHz RFR groups showing PAS-positive basement membrane (double arrows), elongated spermatids (arrows), and acrosomal caps (arrow heads) in some developing spermatids and Leydig cells (red arrows). The stages of seminiferous tubules were labeled. Acute sham (S1): **A**, **E**; acute RFR (RFR1): **B**, **F**; chronic sham (S10): **C**, **G**; chronic RFR (RFR10): **D**, **H**; lumen (L). Scale bars represent 50 µm

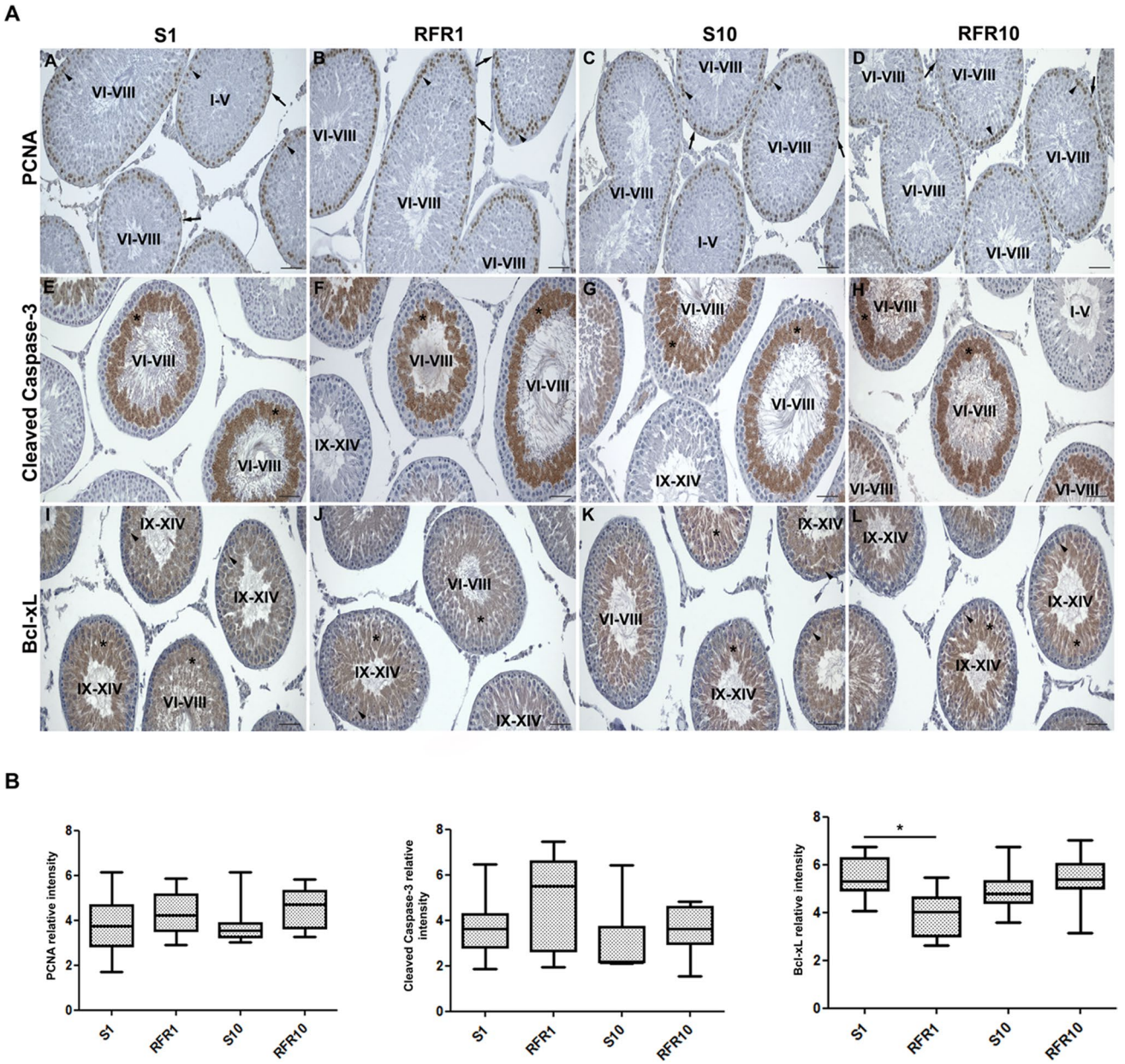
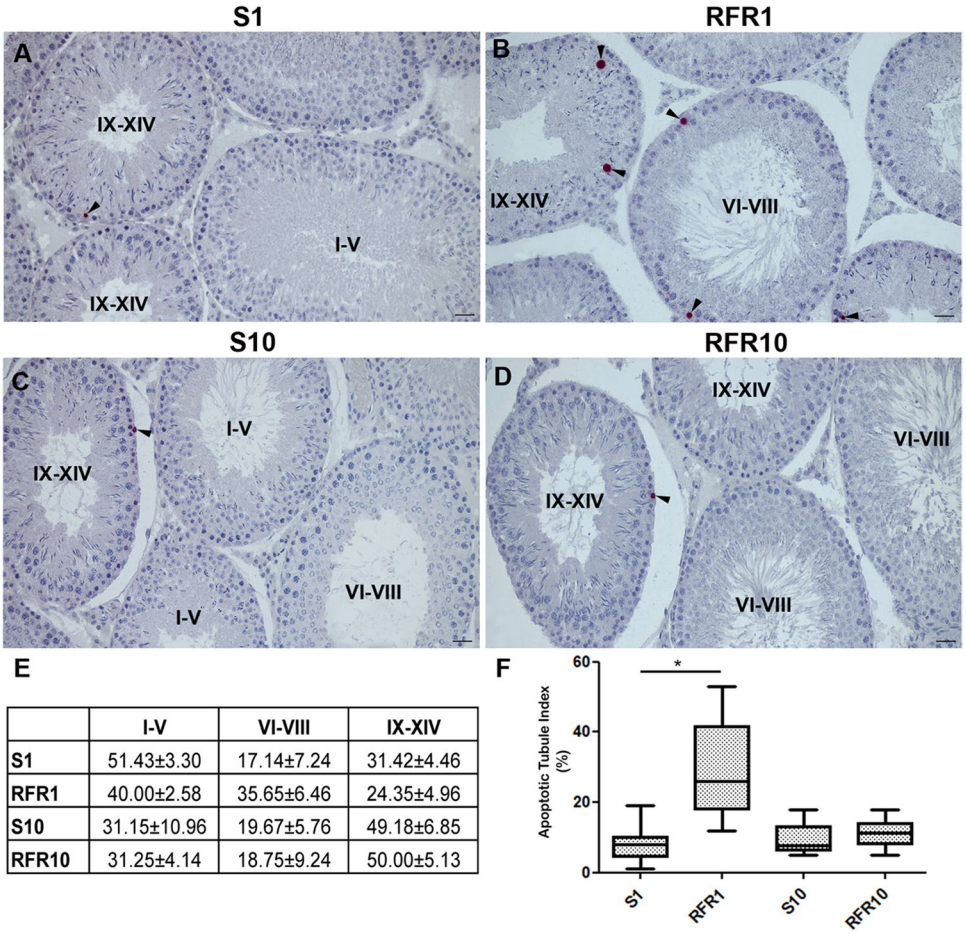


Fig. 3 PCNA (**A**–**D**), cleaved caspase-3 (**E**–**H**), and Bcl-xL (**I**–**L**) immunostainings in rat testicular tissues from sham and 900 MHz RFR groups with labeled seminiferous tubule stages (**A**) and their ImageJ analysis (**B**). Spermatogonial cells (arrows), spermatocytes (arrow heads), and postmeiotic germ cells (asterisks). Acute sham (S1), acute RFR (RFR1), chronic sham (S10), and chronic RFR (RFR10). Scale bars represent 50 µm

in both acute and chronic periods. The results revealed that there was a statistically significant increase in the RFR group in the acute period when compared to the sham group ($p < 0.001$) (Fig. 4F), mostly in VI–VIII seminiferous tubule stages (Fig. 4E). However, no significant difference was observed between sham and RFR groups in the chronic periods (Fig. 4F). There was not any difference by means of specific seminiferous tubule staging (Fig. 4E). TUNEL positive cells have been observed particularly among spermatogonia, spermatocyte, and Leydig cells. In all groups, TUNEL positive cells were observed in all tubule stages. TUNEL positive cells were mostly seen in I–V stages in acute periods and in IX–XIV stages that there should be no maturation-phase spermatids visible, and these tubules should only contain a single population of elongating spermatids in chronic periods (Fig. 4E).



	I-V	VI-VIII	IX-XIV
S1	51.43±3.30	17.14±7.24	31.42±4.46
RFR1	40.00±2.58	35.65±6.46	24.35±4.96
S10	31.15±10.96	19.67±5.76	49.18±6.85
RFR10	31.25±4.14	18.75±9.24	50.00±5.13

Fig. 4 TUNEL analysis for sham and 900 MHz RFR groups are presented. Representative TUNEL stainings (**A**–**D**), percentages of TUNEL positive tubule stages (**E**), and apoptotic tubule indexes (**F**) of acute sham (S1), acute RFR (RFR1), chronic sham (S10), and chronic RFR (RFR10) groups. A statistically significant increase was observed in the acute period after exposure to 900 MHz RFR in rat testis compared to sham group ($p < 0.001$). The results were given as mean ± SEM

Phosphorylation of MAPK Pathway After Exposure to 900 MHz RFR in Acute and Chronic Periods

p-p38 was detected primarily in spermatocytes with a nuclear localization (Fig. 5). Round spermatids, elongated spermatids, and some of the Leydig cells were alsopositively stained. The localization pattern was similar in all groups in acute and chronic periods. However,significant increases in p-p38 immunostaining intensities in RFR groups were observed when compared to shamgroups in both acute ($p < 0.001$) and chronic ($p < 0.001$) periods according to the ImageJ threshold analysis.

Furthermore, p-JNK immunostaining showed a nuclear staining pattern in spermatogonial cells, spermatocytes, the heads of round, and elongated spermatids in some of the seminiferous tubules (Fig. 6). In addition, some of the Leydig cells in the interstitial areas showed strong immunostaining. Even though similar cells were immunopositive with p-JNK, there were significant increases in RFR groups when compared to their sham groups in both acute ($p < 0.001$) and chronic ($p < 0.001$) periods according to the ImageJ threshold analysis as observed for p-p38.

Western blot analysis also supported the data that there were statistically significant increases for p-p38 (40 kDa) and p-JNK (46 kDa) proteins in testicular lysates from RFR groups when compared to sham groups in both acute and chronic periods (Fig. 7).

Discussion

With the development of technology, devices such as mobile phones that emit RFR have been included in our daily life intensively more than before. The mobile phones of today have so many high-tech features that the owners can hardly seem to put them down just for a second. Thus, daily time spent on the usage of mobile phones, which work with RFR, is prolonged. With arising smart mobile phone addiction, it is claimed that RFR may have negative effects on human health such as DNA damage, diminished male fertility, and oxidative stress [11, 46, 59]. Therefore, many studies have been conducted on the biological effects of RFR by using different frequencies, SAR values, durations, and tissues [58, 72–74]. There is also an increased number of studies

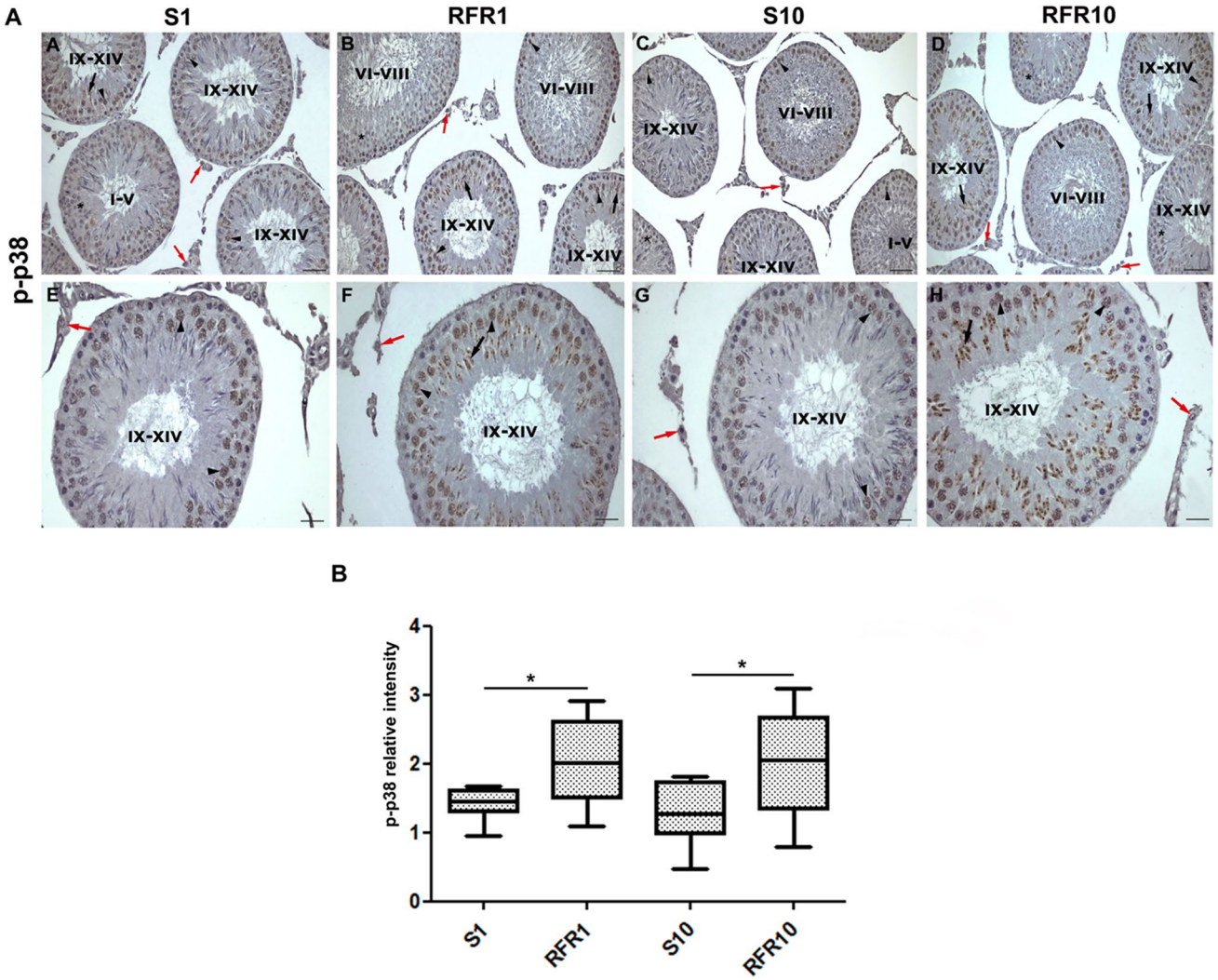


Fig. 5 p-p38immunostainings in rat testicular tissues from sham and 900 MHz RFR groups in both acute and chronic periodswith labeled seminiferous tubule stages (**A**) and their ImageJ analysis (**B**). p-p38 positive spermatocytes (arrow heads), elongated spermatids (arrows), roundspermatids (asterisks), and Leydig cells (red arrows). Acute sham (S1), acute RFR (RFR1), chronic sham (S10),chronic RFR (RFR10), and lumen (L). Scale bars represent 50 µm

investigating the potential effects on the male reproductive system, particularly on testis [75–77]. Some studies clearly indicate that RFR may have negative effects on the testis [75, 76]. Therefore, in our study, we investigated the potential effects of 900 MHz RFR exposure on the rat testicular cell proliferation and apoptosis in line with the activated MAPK signaling pathway by studying SAPKs, p-p38, and p-JNK.

There is an increasing concern in the context of RFR exposure on cell proliferation. Thus, conflicting results in several studies on various tissues have been previously reported [78–80]. For instance, PCNA expression was examined in a single extremely low-frequency electromagnetic field (ELF-EMF) study by applying 4.5 mT-120 Hz ELF-EMF for 50 min/day to the cancer-induced rat liver for 32 days [80]. The study reported that PCNA expression was decreased in cancer and EMF groups compared to the only cancer groups. However, we used normal healthy rat testicular tissues in our study. On the other hand, our both immunohistochemistry and Western blot results supported the data that none of the PCNA localization patterns, expression threshold, or the protein levels were affected among groups due to exposure to 900 MHz RFR suggesting this exposure does not affect the cell proliferation in rat testis in both acute and chronic periods.

Cell proliferation and cell death are essential but opposing cellular processes. However, coordination between these processes is required to keep in balance for normal development and tissue homeostasis. In this context, we investigated testicular cell apoptosis by using cleaved caspase-3, Bcl-xL, and TUNEL analysis. Our results showed that cleaved

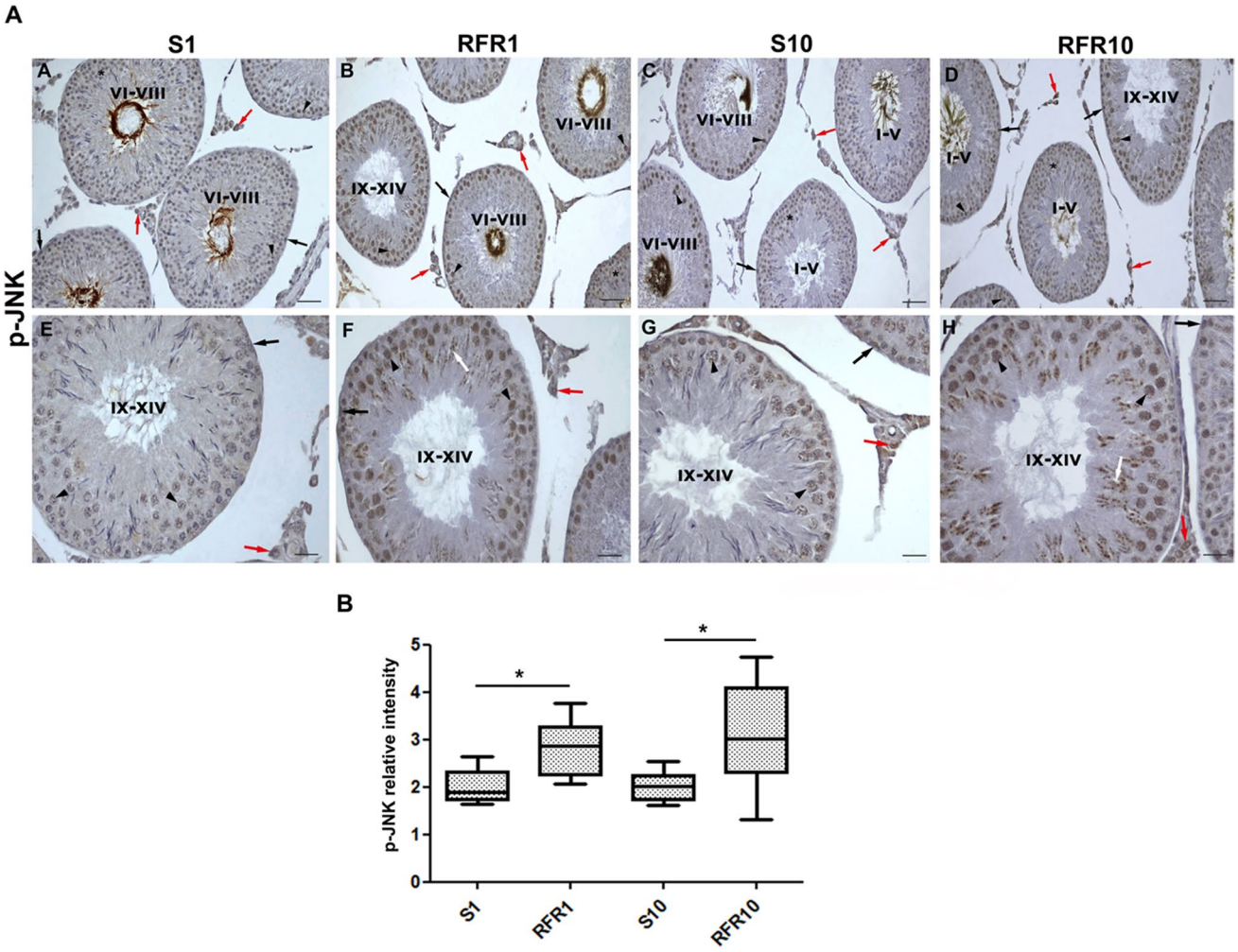


Fig. 6 p-JNK immunostainings in rat testicular tissues from sham and 900 MHz RFR groups in both acute and chronic periods with labeled seminiferous tubule stages (**A**) and their ImageJ analysis (**B**). p-JNK positive spermatogonial cells (arrows), spermatocytes (arrow heads), elongated spermatids (white arrows), round spermatids (asterisks), and Leydig cells (red arrows). Acute sham (S1), acute RFR (RFR1), chronic sham (S10), chronic RFR (RFR10), and lumen (L). Scale bars represent 50 µm

caspase-3 expression was not altered between groups in the acute period, but a significant decrease in the RFR group in the chronic period compared to its sham group was observed by Western blot but not in IHC threshold analysis. We used ImageJ analysis for gathering semiquantitative data from both IHC and Western blot methods. Although both Western blot and IHC rely on the principle of the antibody-antigen interaction, the sample preparations are different. For IHC, it needs to be noted that the tissue samples are sliced, and the limit for the size of samples is 5 µm, which is one of the major disadvantages. In fact, for the first time in literature, we demonstrated the potential effects of 900 MHz RFR exposure in rat testis for the acute period. Guo, L. et al. recently administered 220 MHz RFR to rats for 1 h a day for 30 days (SAR: 0.014 W/kg) and reported that the amount of cleaved caspase-3 stained cells and protein in testis increased significantly in the RFR groups compared to the sham groups [81]. In another study, there was no significant difference in the amount of cleaved caspase-3 stained cells in rat testis, which was applied 900 MHz RFR (SAR: 0.07–0.57 W/kg) for 10 months (2 h/day) compared to the control groups [8]. On the other hand, our data for Bcl-xL protein showed a decreased expression level in the acute period, whereas there was no significant alteration in the chronic period after exposure to 900 MHz RFR. In the literature, studies related to Bcl-xL protein or other antiapoptotic proteins such as Bcl-2 from the same family in the testis are also quite limited related to the effects of RFR exposure. The balance between the antiapoptotic (Bcl-2 and Bcl-xL) and proapoptotic (Bad and Bax) Bcl-2 family proteins regulates cell survival and death [82]. Bcl-xL binds to Bax and consequently inhibits apoptosis [83, 84]. Thus, Bcl-xL and Bcl-2 block Bax translocation to the mitochondria and maintain the mitochondrial membrane potential to prevent

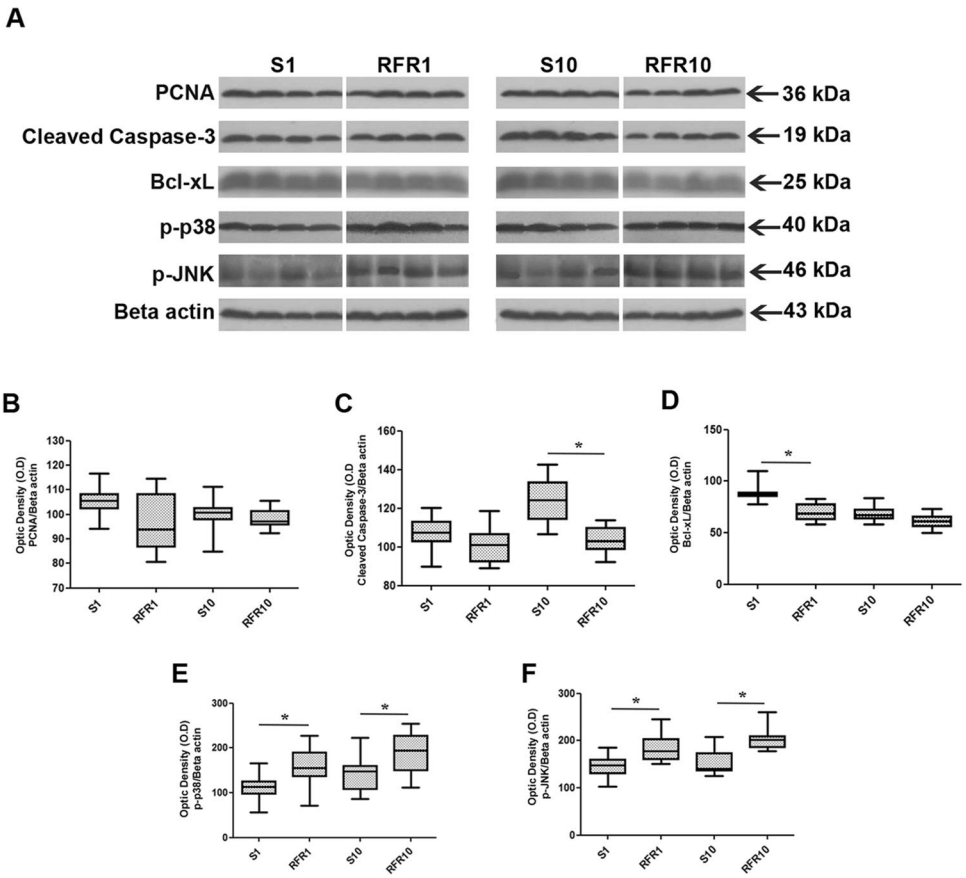


Fig. 7 Western blot analysis of PCNA (36 kDa), cleaved caspase-3 (19 kDa), Bcl-xL (25 kDa), p-p38 (40 kDa), and p-JNK (46 kDa) proteins in the testicular tissues from sham and 900 MHz RFR groups in both acute and chronic periods. The expression of β-actin (43 kDa) was used to confirm equivalent amounts of total proteins loaded per lane. Acute sham (S1), acute RFR (RFR1), chronic sham (S10), and chronic RFR (RFR10)

subsequent apoptosis [84]. In accordance with our chronic period results, it was revealed that there were no significant differences in Bcl-2 expressions in long-term applications in studies in which RFR was applied at 900 MHz, 848.5 MHz, and 2.45 GHz on rat testis [85–87]. On the other hand, it was shown that Bcl-xL and Bcl-2 expressions decreased in long-term applications in two studies conducted in rat and mouse testis under 900 MHz and 2.45 GHz RFR exposures [9, 88]. There are several possible reasons why the aforementioned studies have not produced consistent results with each other such as experimental setup, different RF exposure durations, SAR values, etc.

Furthermore, in our study, the TUNEL method was used to determine whether or not 900 MHz RFR exposure causes apoptosis in rat testis in the acute and chronic periods. According to TUNEL analysis, apoptosis in acute groups was significantly higher in the RFR group than in the sham group, whereas no difference was observed in the chronic groups. The seminiferous tubule staging seems to be similar between groups in chronic periods even though alterations were present in the acute periods. The small discrepancies may be explained by the fact that many stages of the development of the cells cannot be characterized with precision in preparations stained with hematoxylin. In a study conducted on rats, 500 μT and 50 Hz ELF-MF was administered to rats for 4 h/day, 7 days/week, and 4 and 8 weeks. There were no significant differences in the number of TUNEL positive cells in rat testis compared to the sham groups in the 4 and 8 weeks RFR groups [89]. In another study, 900 MHz RFR was administered to rats for 4 h/day for 18 days, and apoptosis was found to be higher in the RFR groups than the sham groups in rat liver [90]. Our TUNEL results obtained in acute and chronic periods are consistent with these studies reporting 900 MHz RFR exposure may increase apoptosis in the acute phase and may not have harmful effects in the chronic periods.

Stress-activated MAP kinases, JNK, and p38 are activated by cell stress-inducing signals. Prolonged activation of JNK and p38 kinases inhibits Bcl-2 and its homologs, such as Bcl-xL, which results in cytochrome c release and the activation of the intrinsic pathway of apoptosis [91]. Pharmacological inhibitors of p38 and JNK affected the expression of Bcl-xL, cytochrome c release, and the fraction of cells undergoing programmed cell death [92]. In our study, p-p38 and p-JNK proteins were examined to determine whether SAPKs involves in the process during 900 MHz RFR application in the rat testis. Our Western blot and IHC results showed that both protein expressions increased after RFR applications in both acute and chronic periods. In the literature, there is only one S-band microwave (S-MW) radiation

study in which p-p38 and p-JNK proteins were studied in the rat testis [93]. Although the electromagnetic wave used in this study is not exactly the same as ours, it is known that 900 MHz is both a radio and a microwave frequency. In that study, rats were exposed to two different doses of microwave radiation (30 mW/cm^2, 100 mW/cm^2) at different time periods as 6 h, 3 days, 7 days, and 14 days. The study reported no significant differences in the expressions of either protein in the 7-day groups. On the other hand, it was observed that there were significant increases in the expressions of both proteins in the 6-h groups in which applied 30 mW/cm^2.

Studies have also demonstrated that expressions of Bcl-2 family proteins is regulated by JNK and ERK signaling [94]. JNK signaling promotes apoptosis via regulating Bcl-2 family proteins [95]. Increased p-p38 and p-JNK protein expressions and also increased number of TUNEL-positive seminiferous tubules were observed in contrast to a decrease in Bcl-xL expression in our acute period groups. Therefore, exposure to 900 MHz RFR in the acute period may inhibit Bcl-xL expression and trigger apoptosis by increasing p-p38 and p-JNK expressions in the rat testis. On the other hand, there were increases in p-p38 and p-JNK protein expressions in our chronic groups, but no changes in Bcl-xL expression or the number of TUNEL-positive seminiferous tubules were observed. This may be related to our experimental timeline. In the chronic periods, we have applied RFR for 5 days/week, not on the weekends. Therefore, possibly the antioxidant defense system of the body eliminated the negative effects of RFR in the long-term 900 MHz RFR application. For our acute periods, there were no 2-day breaks for the weekend since the whole experiment was finalized at the end of the fifth day. In another point of view, an adaptation process may have been developed in chronic period groups. In order to test this, RFR exposure can also be continued on the weekends in subsequent studies to analyze whether this difference is caused by the antioxidant defense system or by an adaptation mechanism. On the other hand, there is another question of whether fertility alters in line with several sperm parameters such as concentration and motility between experimental groups. That is a critical issue in new insight into reproductive health as well as male fertility even though we observed full spermatogenesis in all testicular tissue samples studied. However, detailed studies regarding fertility outcomes need to be further investigated.

In conclusion, our study shows that at low SAR values and less than 2 h a day, exposure to 900 MHz RFR might have negative effects in the rat testis in acute periods, not as much as in chronic periods. Increased expressions of p-p38 and p-JNK support the idea that SAP kinases are activated during 900 MHz RFR exposure. However, detailed molecular mechanisms and protein interactions are needed to be determined during these processes. Therefore, the duration and exposure periods seem to be crucial for heavy mobile phone users and should not be neglected for potential negative health effects.

Acknowledgements This work was supported by a research grant from Akdeniz University, The Scientific Research Projects Coordination Unit (TSA-2018-3739).

Author Contribution LS designed the experiment and interpreted the data; HE, BS, GGT, SO, and LS performed the experiments, collected the data, and analyzed the results; HE and LS wrote the manuscript. All authors edited the manuscript and have given approval for the publication of the present version of this manuscript.

Funding This work was supported by a research grant from Akdeniz University, The Scientific Research Projects Coordination Unit (TSA-2018-3739).

Data Availability The data supporting the findings of this study are available within this article.

Code Availability Not applicable.

Declarations

Ethics Approval All the experimental animal protocols for this study were approved by the Akdeniz University Local Ethics Committee for Animal Experiments (protocol number: 758/2018.10.07).

Consent to Participate Not applicable.

Consent for Publication All authors consent to the publication of the manuscript.

Conflict of Interest The authors declare no competing interests.

References

1. Krause CM, Sillanmaki L, Koivisto M, Haggqvist A, Saarela C, Revonsuo A, Laine M, Hamalainen H. Effects of electromagnetic field emitted by cellular phones on the EEG during a memory task. Neuroreport. 2000;11(4):761–4.
2. Albertini A, Zucchini P, Noera G, Cadossi R, Pace Napoleone C, Pierangeli A. Protective effect of low frequency low energy pulsing electromagnetic fields on acute experimental myocardial infarcts in rats. Bioelectromagnetics. 1999;20(6):372–7.
3. Loftis M. Sources of noise-induced hearing loss. AAOHN J. 2007;55(11):476.
4. Hardell L. World Health Organization, radiofrequency radiation and health - a hard nut to crack (Review). Int J Oncol. 2017;51(2):405–13.
5. Hardell L, Carlberg M, Soderqvist F, Hansson MK. Meta-analysis of long-term mobile phone use and the association with brain tumours. Int J Oncol. 2008;32(5):1097–103.
6. Hardell L, Koppel T, Carlberg M, Ahonen M, Hedendahl L. Radiofrequency radiation at Stockholm Central Railway Station in Sweden and some medical aspects on public exposure to RF fields. Int J Oncol. 2016;49(4):1315–24.
7. Zhang KY, Hui X, Du L, Xing JL, Zhang B, Bai QS, Xu YQ, Zhou YC, Zhang JP, Zhou Y, Ding GR. Enhancement of X-ray induced apoptosis by mobile phone-like radio-frequency electromagnetic

fields in mouse spermatocyte-derived cells. Int J Environ Res Public Health. 2017;14(6):616.
8. Dasdag S, Akdag MZ, Ulukaya E, Uzunlar AK, Yegin D. Mobile phone exposure does not induce apoptosis on spermatogenesis in rats. Arch Med Res. 2008;39(1):40–4.
9. Shahin S, Singh SP, Chaturvedi CM. 2.45 GHz microwave radiation induced oxidative and nitrosative stress mediated testicular apoptosis: involvement of a p53 dependent bax-caspase-3 mediated pathway. Environ Toxicol. 2018;33(9):931–45.
10. Hardell L, Carlberg M, Hansson MK. Pooled analysis of case-control studies on malignant brain tumours and the use of mobile and cordless phones including living and deceased subjects. Int J Oncol. 2011;38(5):1465–74.
11. Pandey N, Giri S, Das S, Upadhaya P. Radiofrequency radiation (900 MHz)-induced DNA damage and cell cycle arrest in testicular germ cells in swiss albino mice. Toxicol Ind Health. 2017;33(4):373–84.
12. Odacı E, Hancı H, Yuluğ E, Türedi S, Aliyazıcıoğlu Y, Kaya H, Çolakoğlu S. Effects of prenatal exposure to a 900 MHz electromagnetic field on 60-day-old rat testis and epididymal sperm quality. Biotech Histochem. 2016;91(1):9–19.
13. Kesari KK, Kumar S, Behari J. 900-MHz microwave radiation promotes oxidation in rat brain. Electromagn Biol Med. 2011;30(4):219–34.
14. Abolfathi AA, Mohajeri D, Rezaie A, Nazeri M. Protective effects of green tea extract against hepatic tissue injury in streptozotocin-induced diabetic rats. Evid Based Complement Alternat Med. 2012;2012:740671.
15. Aitken RJ, Roman SD. Antioxidant systems and oxidative stress in the testes. Oxidative Med Cell Longev. 2008;1(1):15–24.
16. Maskey D, Kim M, Aryal B, Pradhan J, Choi IY, Park KS, Son T, Hong SY, Kim SB, Kim HG, Kim MJ. Effect of 835 MHz radiofrequency radiation exposure on calcium binding proteins in the hippocampus of the mouse brain. Brain Res. 2010;1313:232–41.
17. Aitken RJ, De Iuliis GN, Finnie JM, Hedges A, McLachlan RI. Analysis of the relationships between oxidative stress, DNA damage and sperm vitality in a patient population: development of diagnostic criteria. Hum Reprod. 2010;25(10):2415–26.
18. Naziroglu M. New molecular mechanisms on the activation of TRPM2 channels by oxidative stress and ADP-ribose. Neurochem Res. 2007;32(11):1990–2001.
19. Naziroglu M. TRPM2 cation channels, oxidative stress and neurological diseases: where are we now? Neurochem Res. 2011;36(3):355–66.
20. Naziroglu M. Molecular role of catalase on oxidative stress-induced Ca(2+) signaling and TRP cation channel activation in nervous system. J Recept Signal Transduct Res. 2012;32(3):134–41.
21. Bennett D, Janes M, Sati L, Sakkas D, Huszar G. Oxidative processes and paternal contribution of spermatozoa: relationship between reactive oxygen species (ROS) production and unexplained male infertility. Fertil Steril. 2005;84:S76–S7.
22. Celik-Ozenci C, Sati L, Huszar G. *Role of sperm-hyaluronic acid binding in the evaluation and treatment of subfertile men with ROS-affected semen*. In: in *male infertility*. Cham: Springer; 2020. p. 695–706.
23. Aitken RJ, Fisher HM, Fulton N, Gomez E, Knox W, Lewis B, Irvine S. Reactive oxygen species generation by human spermatozoa is induced by exogenous NADPH and inhibited by the flavoprotein inhibitors diphenylene iodonium and quinacrine. Mol Reprod Dev. 1997;47(4):468–82.
24. Agarwal A, Makker K, Sharma R. Clinical relevance of oxidative stress in male factor infertility: an update. Am J Reprod Immunol. 2008;59(1):2–11.
25. Tremellen K. Oxidative stress and male infertility--a clinical perspective. Hum Reprod Update. 2008;14(3):243–58.
26. Zalata A, El-Samanoudy AZ, Shaalan D, El-Baiomy Y, Mostafa T. In vitro effect of cell phone radiation on motility, DNA fragmentation and clusterin gene expression in human sperm. Int J Fertil Steril. 2015;9(1):129–36.
27. Agarwal A, Deepinder F, Sharma RK, Ranga G, Li J. Effect of cell phone usage on semen analysis in men attending infertility clinic: an observational study. Fertil Steril. 2008;89(1):124–8.
28. Kumar S, Nirala JP, Behari J, Paulraj R. Effect of electromagnetic irradiation produced by 3G mobile phone on male rat reproductive system in a simulated scenario. Indian J Exp Biol. 2014;52(9):890–7.
29. Yan JG, Agresti M, Bruce T, Yan YH, Granlund A, Matloub HS. Effects of cellular phone emissions on sperm motility in rats. Fertil Steril. 2007;88(4):957–64.
30. Kesari KK, Kumar S, Behari J. Mobile phone usage and male infertility in Wistar rats. Indian J Exp Biol. 2010;48(10):987–92.
31. Adams JA, Galloway TS, Mondal D, Esteves SC, Mathews F. Effect of mobile telephones on sperm quality: a systematic review and meta-analysis. Environ Int. 2014;70:106–12.
32. Kilgallon SJ, Simmons LW. Image content influences men's semen quality. Biol Lett. 2005;1(3):253–5.
33. Slater AF, Stefan C, Nobel I, van den Dobbelsteen DJ, Orrenius S. Intracellular redox changes during apoptosis. Cell Death Differ. 1996;3(1):57–62.
34. Davis RJ. The mitogen-activated protein kinase signal transduction pathway. J Biol Chem. 1993;268(20):14553–6.
35. Chang L, Karin M. Mammalian MAP kinase signalling cascades. Nature. 2001;410(6824):37–40.
36. McCubrey JA, Lahair MM, Franklin RA. Reactive oxygen species-induced activation of the MAP kinase signaling pathways. Antioxid Redox Signal. 2006;8(9-10):1775–89.
37. Dent P, Yacoub A, Fisher PB, Hagan MP, Grant S. MAPK pathways in radiation responses. Oncogene. 2003;22(37):5885–96.
38. Engelberg D. Stress-activated protein kinases-tumor suppressors or tumor initiators? Semin Cancer Biol. 2004;14(4):271–82.
39. Kyriakis JM, Avruch J. Mammalian mitogen-activated protein kinase signal transduction pathways activated by stress and inflammation. Physiol Rev. 2001;81(2):807–69.
40. Reddy KB, Nabha SM, Atanaskova N. Role of MAP kinase in tumor progression and invasion. Cancer Metastasis Rev. 2003;22(4):395–403.
41. Wilkinson MG, Millar JB. Control of the eukaryotic cell cycle by MAP kinase signaling pathways. FASEB J. 2000;14(14):2147–57.
42. Johnson GL, Lapadat R. Mitogen-activated protein kinase pathways mediated by ERK, JNK, and p38 protein kinases. Science. 2002;298(5600):1911–2.
43. Navarro R, Busnadiego I, Ruiz-Larrea MB, Ruiz-Sanz JI. Superoxide anions are involved in doxorubicin-induced ERK activation in hepatocyte cultures. Ann N Y Acad Sci. 2006;1090:419–28.
44. Maundrell K, Antonsson B, Magnenat E, Camps M, Muda M, Chabert C, Gillieron C, Boschert U, Vial-Knecht E, Martinou JC, Arkinstall S. Bcl-2 undergoes phosphorylation by c-Jun N-terminal kinase/stress-activated protein kinases in the presence of the constitutively active GTP-binding protein Rac1. J Biol Chem. 1997;272(40):25238–42.
45. Yu C, Minemoto Y, Zhang J, Liu J, Tang F, Bui TN, Xiang J, Lin A. JNK suppresses apoptosis via phosphorylation of the proapoptotic Bcl-2 family protein BAD. Mol Cell. 2004;13(3):329–40.
46. Yu G, Tang Z, Chen H, Chen Z, Wang L, Cao H, Wang G, Xing J, Shen H, Cheng Q. Long-term exposure to 4G smartphone radiofrequency electromagnetic radiation diminished male reproductive potential by directly disrupting Spock3–MMP2-BTB axis in the testes of adult rats. Sci Total Environ. 2020;698:133860.
47. Srivastava RK, Mi QS, Hardwick JM, Longo DL. Deletion of the loop region of Bcl-2 completely blocks paclitaxel-induced apoptosis. Proc Natl Acad Sci U S A. 1999;96(7):3775–80.

48. Nebreda AR, Porras A. p38 MAP kinases: beyond the stress response. Trends Biochem Sci. 2000;25(6):257–60.
49. Takenobu H, Yamazaki A, Hirata M, Umata T, Mekada E. The stress- and inflammatory cytokine-induced ectodomain shedding of heparin-binding epidermal growth factor-like growth factor is mediated by p38 MAPK, distinct from the 12-O-tetradecanoylphorbol-13-acetate- and lysophosphatidic acid-induced signaling cascades. J Biol Chem. 2003;278(19):17255–62.
50. Abe MK, Kuo WL, Hershenson MB, Rosner MR. Extracellular signal-regulated kinase 7 (ERK7), a novel ERK with a C-terminal domain that regulates its activity, its cellular localization, and cell growth. Mol Cell Biol. 1999;19(2):1301–12.
51. De Cesaris P, Starace D, Starace G, Filippini A, Stefanini M, Ziparo E. Activation of Jun N-terminal kinase/stress-activated protein kinase pathway by tumor necrosis factor alpha leads to intercellular adhesion molecule-1 expression. J Biol Chem. 1999;274(41):28978–82.
52. Shiraishi K, Yoshida K, Fujimiya T, Naito K. Activation of mitogen activated protein kinases and apoptosis of germ cells after vasectomy in the rat. J Urol. 2002;168(3):1273–8.
53. Gupta S, Barrett T, Whitmarsh AJ, Cavanagh J, Sluss HK, Derijard B, Davis RJ. Selective interaction of JNK protein kinase isoforms with transcription factors. EMBO J. 1996;15(11):2760–70.
54. De Cesaris P, Starace D, Riccioli A, Padula F, Filippini A, Ziparo E. Tumor necrosis factor-alpha induces interleukin-6 production and integrin ligand expression by distinct transduction pathways. J Biol Chem. 1998;273(13):7566–71.
55. Crepieux P, Marion S, Martinat N, Fafeur V, Vern YL, Kerboeuf D, Guillou F, Reiter E. The ERK-dependent signalling is stage-specifically modulated by FSH, during primary Sertoli cell maturation. Oncogene. 2001;20(34):4696–709.
56. Sun QY, Breitbart H, Schatten H. Role of the MAPK cascade in mammalian germ cells. Reprod Fertil Dev. 1999;11(7-8):443–50.
57. Sengupta P. The laboratory rat: relating its age with human's. Int J Prev Med. 2013;4(6):624.
58. Bodera P, Antkowiak B, Paluch M, Sirav B, Siwicki AK, Stankiewicz W. The effects of radio-frequency radiation (RFR) exposure on the analgesic efficacy of morphine in healthy rats and rats with inflammation. Int J Occup Med Environ Health. 2019;32(4):465–74.
59. Alkis ME, Bilgin HM, Akpolat V, Dasdag S, Yegin K, Yavas MC, Akdag MZ. Effect of 900-, 1800-, and 2100-MHz radiofrequency radiation on DNA and oxidative stress in brain. Electromagn Biol Med. 2019;38(1):32–47.
60. Ammari M, Gamez C, Lecomte A, Sakly M, Abdelmelek H, De Seze R. GFAP expression in the rat brain following sub-chronic exposure to a 900 MHz electromagnetic field signal. Int J Radiat Biol. 2010;86(5):367–75.
61. Burkhardt M, Spinelli Y, Kuster N. Exposure setup to test effects of wireless communications systems on the CNS. Health Phys. 1997;73(5):770–8.
62. Fritze K, Wiessner C, Kuster N, Sommer C, Gass P, Hermann D, Kiessling M, Hossmann K-A. Effect of global system for mobile communication microwave exposure on the genomic response of the rat brain. Neuroscience. 1997;81(3):627–39.
63. Schönborn F, Poković K, Kuster N. Dosimetric analysis of the carousel setup for the exposure of rats at 1.62 GHz. Bioelectromagnetics. 2004;25(1):16–26.
64. Weiland T. A discretization model for the solution of Maxwell's equations for six-component fields. Archiv Elektronik und Uebertragungstechnik. 1977;31:116–20.
65. Razi-Kazemi AA, Hajian M. Probabilistic assessment of ground potential rise using finite integration technique. IEEE Trans Power Deliv. 2018;33(5):2452–61.
66. Gabriel S, Lau R, Gabriel C. The dielectric properties of biological tissues: II. Measurements in the frequency range 10 Hz to 20 GHz. Phys Med Biol. 1996;41(11):2251.
67. Abdilla L, Sammut C, Mangion LZ. Dielectric properties of muscle and liver from 500 MHz–40 GHz. Electromagn Biol Med. 2013;32(2):244–52.
68. Celik-Ozenci C, Tasatargil A, Tekcan M, Sati L, Gungor E, Isbir M, Demir R. Effects of abamectin exposure on male fertility in rats: potential role of oxidative stress-mediated poly (ADP-ribose) polymerase (PARP) activation. Regul Toxicol Pharmacol. 2011;61(3):310–7.
69. Leblond C, Clermont Y. Definition of the stages of the cycle of the seminiferous epithelium in the rat. Ann N Y Acad Sci. 1952;55(4):548–73.
70. Creasy DM. Evaluation of testicular toxicity in safety evaluation studies: the appropriate use of spermatogenic staging. Toxicol Pathol. 1997;25(2):119–31.
71. Hess RA, Linder RE, Strader LF, Perreault SD. Acute effects and long-term sequelae of 1, 3-dinitrobenzene on male reproduction in the rat ii. quantitative and qualitative histopathology of the testis. J Androl. 1988;9(5):327–42.
72. Dasdag S, Taş M, Akdag MZ, Yegin K. Effect of long-term exposure of 2.4 GHz radiofrequency radiation emitted from Wi-Fi equipment on testes functions. Electromagn Biol Med. 2015;34(1):37–42.
73. Gökçek-Saraç Ç, Er H, Kencebay Manas C, Kantar Gok D, Özen Ş, Derin N. Effects of acute and chronic exposure to both 900 MHz and 2100 MHz electromagnetic radiation on glutamate receptor signaling pathway. Int J Radiat Biol. 2017;93(9):980–9.
74. Soffritti M, Giuliani L. The carcinogenic potential of non-ionizing radiations: the cases of S-50 Hz MF and 1.8 GHz GSM radiofrequency radiation. Basic Clin Pharmacol Toxicol. 2019;125:58–69.
75. Gautam R, Singh KV, Nirala J, Murmu NN, Meena R, Rajamani P. Oxidative stress-mediated alterations on sperm parameters in male Wistar rats exposed to 3G mobile phone radiation. Andrologia. 2019;51(3):e13201.
76. Kuzay D, Ozer C, Sirav B, Canseven A, Seyhan N. Oxidative effects of extremely low frequency magnetic field and radio frequency radiation on testes tissues of diabetic and healthy rats. Bratisl Lek Listy. 2017;118(5):278–82.
77. Lin Y-Y, Wu T, Liu J-Y, Gao P, Li K-C, Guo Q-Y, Yuan M, Lang H-Y, Zeng L-H, Guo G-Z. 1950MHz Radio frequency electromagnetic radiation inhibits testosterone secretion of mouse Leydig cells. Int J Environ Res Public Health. 2018;15(1):17.
78. Kumar G, McIntosh RL, Anderson V, McKenzie RJ, Wood AW. A genotoxic analysis of the hematopoietic system after mobile phone type radiation exposure in rats. Int J Radiat Biol. 2015;91(8):664–72.
79. Xu F, Bai Q, Zhou K, Ma L, Duan J, Zhuang F, Xie C, Li W, Zou P, Zhu C. Age-dependent acute interference with stem and progenitor cell proliferation in the hippocampus after exposure to 1800 MHz electromagnetic radiation. Electromagn Biol Med. 2017;36(2):158–66.
80. Jiménez-García MN, Arellanes-Robledo J, Aparicio-Bautista DI, Rodríguez-Segura MÁ, Villa-Treviño S, Godina-Nava JJ. Antiproliferative effect of extremely low frequency electromagnetic field on preneoplastic lesions formation in the rat liver. BMC Cancer. 2010;10(1):1–12.
81. Guo L, Lin J-J, Xue Y-Z, An G-Z, Zhang J-P, Zhang K-Y, He W, Wang H, Li W, Ding G-R. Effects of 220 MHz pulsed modulated radiofrequency field on the sperm quality in rats. Int J Environ Res Public Health. 2019;16(7):1286.
82. Zhao H, Yenari MA, Cheng D, Sapolsky RM, Steinberg GK. Bcl-2 overexpression protects against neuron loss within the ischemic margin following experimental stroke and inhibits

cytochrome c translocation and caspase-3 activity. J Neurochem. 2003;85(4):1026–36.
83. Hou J, Wang S, Chen Shang Y, Zhong Chong Z, Maiese K. Erythropoietin employs cell longevity pathways of SIRT1 to foster endothelial vascular integrity during oxidant stress. Curr Neurovasc Res. 2011;8(3):220–35.
84. Koh P-O. Nicotinamide attenuates the ischemic brain injury-induced decrease of Akt activation and Bad phosphorylation. Neurosci Lett. 2011;498(2):105–9.
85. Lee HJ, Pack JK, Kim TH, Kim N, Choi SY, Lee JS, Kim SH, Lee YS. The lack of histological changes of CDMA cellular phone-based radio frequency on rat testis. Bioelectromagnetics. 2010;31(7):528–34.
86. Saygin M, Caliskan S, Karahan N, Koyu A, Gumral N, Uguz A. Testicular apoptosis and histopathological changes induced by a 2.45 GHz electromagnetic field. Toxicol Ind Health. 2011;27(5):455–63.
87. Yilmaz F, Dasdag S, Akdag MZ, Kilinc N. Whole-body exposure of radiation emitted from 900 MHz mobile phones does not seem to affect the levels of anti-apoptotic bcl-2 protein. Electromagn Biol Med. 2008;27(1):65–72.
88. Ma H, Cao X, Ma X, Chen J, Chen J, Yang H, Liu Y. Protective effect of Liuweidihuang pills against cellphone electromagnetic radiation-induced histomorphological abnormality, oxidative injury, and cell apoptosis in rat testes. Zhonghua nan ke xue=Natl J Androl. 2015;21(8):737–41.
89. Duan W, Liu C, Wu H, Chen C, Zhang T, Gao P, Luo X, Yu Z, Zhou Z. Effects of exposure to extremely low frequency magnetic fields on spermatogenesis in adult rats. Bioelectromagnetics. 2014;35(1):58–69.
90. Ma H, Ma Z, Wang G, Song C, Ma X, Cao X, Zhang G. Impacts of exposure to 900 MHz mobile phone radiation on liver function in rats. Zhongguo Ying Yong Sheng li xue za zhi= Zhongguo Yingyong Shenglixue Zazhi= Chinese. J Appl Physiol. 2015;31(6):567–71.
91. Tobiume K, Matsuzawa A, Takahashi T, Nishitoh H, Ki M, Takeda K, Minowa O, Miyazono K, Noda T, Ichijo H. ASK1 is required for sustained activations of JNK/p38 MAP kinases and apoptosis. EMBO Rep. 2001;2(3):222–8.
92. Gabryel B, Liber S. Metformin limits apoptosis in primary rat cortical astrocytes subjected to oxygen and glucose deprivation. Folia Neuropathol. 2018;56:328–36.
93. Wu H, Wang D, Meng Y, Ning H, Liu X, Xie Y, Cui L, Wang S, Xu X, Peng R. Activation of TLR signalling regulates microwave radiation-mediated impairment of spermatogenesis in rat testis. Andrologia. 2018;50(1):e12828.
94. Guan Q-H, Pei D-S, Zhang Q-G, Hao Z-B, Xu T-L, Zhang G-Y. The neuroprotective action of SP600125, a new inhibitor of JNK, on transient brain ischemia/reperfusion-induced neuronal death in rat hippocampal CA1 via nuclear and non-nuclear pathways. Brain Res. 2005;1035(1):51–9.
95. Jeong H-S, Choi H-Y, Choi T-W, Kim B-W, Kim J-H, Lee E-R, Cho S-G. Differential regulation of the antiapoptotic action of B-cell lymphoma 2 (Bcl-2) and B-cell lymphoma extra long (Bcl-xL) by c-Jun N-terminal protein kinase (JNK) 1-involved pathway in neuroglioma cells. Biol Pharm Bull. 2008;31(9):1686–90.

Publisher's Note Springer Nature remains neutral with regard to jurisdictional claims in published maps and institutional affiliations.